LBNL-42021
Preprint

ERNEST ORLANDO LAWRENCE BERKELEY NATIONAL LABORATORY

The Near Ultraviolet Dissociation Dynamics of Azomethane: Correlated V-T Energy Disposal and Product Appearance Times

Allan S. Bracker, Simon W. North,
Arthur G. Suits, and Yuan T. Lee

Chemical Sciences Division

June 1998
Submitted to
Journal of Chemical Physics

REFERENCE COPY
Does Not
Circulate
Bldg. 50 Library - Ref.
Lawrence Berkeley National Laboratory
LBNL-42021
Copy 1

DISCLAIMER

This document was prepared as an account of work sponsored by the United States Government. While this document is believed to contain correct information, neither the United States Government nor any agency thereof, nor the Regents of the University of California, nor any of their employees, makes any warranty, express or implied, or assumes any legal responsibility for the accuracy, completeness, or usefulness of any information, apparatus, product, or process disclosed, or represents that its use would not infringe privately owned rights. Reference herein to any specific commercial product, process, or service by its trade name, trademark, manufacturer, or otherwise, does not necessarily constitute or imply its endorsement, recommendation, or favoring by the United States Government or any agency thereof, or the Regents of the University of California. The views and opinions of authors expressed herein do not necessarily state or reflect those of the United States Government or any agency thereof or the Regents of the University of California.

LBNL-42021

The Near Ultraviolet Dissociation Dynamics of Azomethane: Correlated V-T Energy Disposal and Product Appearance Times

Allan S. Bracker, Simon W. North,
Arthur G. Suits, and Yuan T. Lee

Chemical Sciences Division
Ernest Orlando Lawrence Berkeley National Laboratory
University of California
Berkeley, California 94720

June 1998

This work was supported by the Director, Office of Energy Research, Office of Basic Energy Sciences, Chemical Sciences Division, of the U.S. Department of Energy under Contract No. DE-AC03-76SF00098.

Submitted to Journal of Chemical Physics

The near ultraviolet dissociation dynamics of azomethane: Correlated V-T energy disposal and product appearance times

Allan S. Bracker[a,b], Simon W. North[c], Arthur G. Suits[b] and Yuan T. Lee[a,b,d]

[a] *Department of Chemistry, University of California, Berkeley, CA 94720*

[b] *Chemical Sciences Division, Ernest Orlando Lawrence Berkeley National Laboratory, Berkeley, CA 94720*

[c] *Department of Chemistry, Texas A&M University, P.O. Box 30012, College Station, TX 77842*

[d] *Academia Sinica, Nankang, Taipei 11529, Taiwan*

Abstract

We have measured the translational energy release for methyl radical photofragments with zero and one quantum of umbrella vibration, which were produced by the ultraviolet dissociation of azomethane. Translational energy distributions exhibit bimodal structure and are similar for both methyl radical vibrational states and for two dissociation wavelengths (355 nm and 330 nm). Compared to earlier non-state-selective measurements, these distributions exhibit a stronger preference for high kinetic energies. We have also observed that the appearance times for both methyl radical vibrational states are fast compared to the experimental time resolution, thus resolving an outstanding mechanistic disagreement. These observations are consistent with a previously proposed mechanism in which a concerted three-body dissociation follows randomization of parent internal energy.

I. INTRODUCTION

Azomethane photodissociation in the near ultraviolet has recently received well-deserved attention because of the richness of the resulting three-body dissociation dynamics. Following optical excitation to the first excited singlet state, the process

$$CH_3N_2CH_3 \longrightarrow 2CH_3 + N_2 \tag{1}$$

is thought to occur on the ground electronic state following internal conversion [1,2]. The central dynamical questions concern the timing of bond breakage and the partitioning of energy between the fragments' internal modes and translation. This study addresses both of these issues for the subset of methyl radical fragments with little or no vibrational energy.

Fig. 1 shows a schematic potential energy diagram for azomethane, adapted from the recent *ab initio* study by Liu *et al.* [1]. Photon absorption in the mid-300 nm region excites molecules from the S_0 ground state (^1A_g) to the first excited singlet state S_1 (^1B_g), promoting a nitrogen nonbonding electron to an N–N pi-antibonding orbital. This transition results in a weak diffuse feature ($\sigma = 2\times10^{-20}$ cm^2) in the absorption spectrum, centered at 360 nm [3–5]. Of the first four excited electronic states (two singlet, two triplet), only the second triplet state correlates to reaction products in their ground electronic states, thus nonadiabatic processes must play a role in the production of ground state reaction products produced by excitation to the S_1 state.

Using Coherent Anti-Stokes Raman Spectroscopy, Weisman *et al.* [6,7] initiated the present round of investigations into azomethane dissociation dynamics with a study of the methyl and nitrogen fragment appearance times and quantum state populations. They reported that methyl radicals with one quantum of umbrella vibration (ν_2) appeared in less than one nanosecond, while nonvibrating methyl radicals appeared with a 5.6 ns appearance time. They concluded that the reaction must occur in a stepwise manner, producing two distinct types of methyl radicals. The former were assigned to an impulsive primary dissociation, while the latter were assigned to a statistical secondary dissociation of the

remaining methyldiazenyl radical (CH_3N_2). This interpretation relied primarily on the disparate appearance times of the two vibrational quantum states but was also consistent with the measured vibrational and rotational product state distributions.

A different interpretation emerged from the work of North *et al.* [2], who used photofragment translational spectroscopy to measure recoil energy and angular distributions of the methyl and nitrogen products. They found that the photofragment angular distribution for the primary step was isotropic, within experimental uncertainty. This observation is consistent with a long-lived azomethane excited state, though it could also be explained by a recoil velocity vector near the 'magic angle' (54.7°) with respect to the transition moment. In contrast, the secondary recoil (for CH_3N_2 dissociation) was strongly anisotropic with respect to the primary velocity vector, indicating rapid secondary dissociation. When considered together, these angular distributions support the assignment of statistical and rapid (impulsive) dissociations to the first and second steps, respectively, which is the reverse of the assignment by Weisman *et al.* Finally, a bimodal methyl translational energy distribution demonstrated explicitly the existence of two dynamically distinct methyl radicals.

North *et al.* proposed that after optical excitation ($S_0 \rightarrow S_1$), rapid internal conversion places the molecule in a highly vibrationally excited state of the S_0 potential energy surface. On a timescale longer than the azomethane rotational period, enough vibrational energy accumulates in one CN bond for the first methyl to overcome a dissociation energy of roughly 50 kcal/mol, with little or no exit barrier. The remaining CH_3N_2 radical is bound by less than 2 kcal/mol and rapidly dissociates into a second methyl radical and a nitrogen molecule, which are repelled by a large exit barrier (25–30 kcal/mol). Based on a common empirical defintion [8], they identified the asymmetric loss of both methyls during less than a CH_3N_2 rotational period as a 'concerted' process [8].

This mechanism is largely consistent with the *ab initio* potential energy surface calculated by Liu *et al.* [1]. They found that internal conversion is likely to occur through a combination of increasing CNN angle and CNNC torsion, which brings the S_0 and S_1 surfaces close together in energy. Although a symmetric (synchronous) dissociative pathway on the

S_0 surface was calculated to be lower in energy than the concerted pathway, the concerted mechanism was favored when free energy was considered. With a zero-point-corrected dissociation barrier of only 0.2 kcal/mol, one would expect the CH_3N_2 radical to have a lifetime shorter than its rotational period.

Although the *ab initio* results favor the interpretation of North *et al.*, the disagreement with the results of Weisman *et al.* has not been resolved. More detailed measurements of energy partitioning should help to secure a correct mechanistic interpretation. A quantum-state-selective study by Fairbrother *et al.* [9] has made some progress in this direction. By extracting average energies from the width of methyl ion peaks in a time-of-flight mass spectrum, they concluded that vibrationless methyl radicals are present only in the fast component of the translational energy distribution. This surprising result may suggest that the translational-vibrational partitioning is highly state specific.

Gejo *et al.* [10] have studied azomethane dissociation at higher energy (193 nm). At this wavelength, a different electronic state is accessed, and it is less clear whether the dissociation is direct or occurs following internal conversion to the ground state. Their observation of nearly equivalent methyl kinetic energy release and an anisotropic secondary angular distribution pointed to either a concerted or symmetric (synchronous) mechanism. Given the considerably higher available energy, it was not surprising that a stepwise mechanism was easily ruled out.

A great deal has already been learned about the gas-phase dissociation of azomethane, but as a prototype for three-body dissociation of symmetric molecules, the picture remains naggingly incomplete. This study has two objectives. First, we reinvestigate the issue of methyl radical appearance times in an effort to resolve the outstanding contradiction between the results of Weisman *et al.* and North *et al.* Second, we use an experimental approach similar to Fairbrother *et al.* to extract translational energy distributions for vibrationless and umbrella-excited methyl radicals. This additional detail allows a critical comparison with the earlier non-state resolved measurements [2].

II. EXPERIMENT

The experimental technique combines Resonance-enhanced Multiphoton Ionization (REMPI) as a state-selective photofragment probe, with core-sampled Time-of-flight Mass Spectrometry (TOFMS) for kinetic energy and mass resolution. A pulsed supersonic molecular beam of 10% azomethane in helium was crossed within a set of ion extraction optics by one or more lasers. The experiment was carried out under conditions which minimize clustering. In the two laser experiment, photolysis was initiated with an 8 ns pulse of the Nd:YAG laser third harmonic (355 nm). The REMPI probe pulse near 330 nm was the doubled output of an Nd:YAG-pumped dye laser. In a second set of measurements, a single laser was used to study the dissociation process at the wavelength of the probe laser.

Focussing conditions for the dissociation and probe lasers were chosen with consideration of the low azomethane absorption cross section ($\sigma = 1.9\times10^{-20}$ cm^2) and the relative ease of multiphoton absorption. While multiphoton processes are less important at low power densities, we were unable to operate at such low powers that these effects were eliminated, while still producing practical signal count rates. In particular, azomethane, methyldiazenyl and methyl ions appeared in the mass spectrum as a consequence of absorbing three or more photons from either the dissociation or probe lasers. These processes were addressed by Fairbrother *et al.*, and we consider them in more detail in a separate publication [11]. In order to maximize the desired signal while keeping the nonresonantly-produced ions at a workable level, we used a laser spot size of 0.5 mm^2 at the interaction region. This relatively large spot kept the power density acceptably low (despite pulse energies as high as 5 mJ), while increasing the interaction volume and thus the number of molecules in the sample.

For detection of methyl radicals, we used the well-known 2+1 REMPI scheme through the $3p\ ^2A_2''$ Rydberg state [12]. The transition between vibrationless methyl states lies at 333.4 nm (designated 0_0^0) while that between states with a single quantum of umbrella vibration (v_2=1) lies at 329.4 nm (designated 2_1^1). Due to efficient predissociation, individual rotational lines are not resolved and higher vibrational levels were too weak to observe. In

detecting methyl radicals with this scheme, we positioned the laser frequency at the maximum of the REMPI peaks, which corresponds to the narrow cluster of broadened Q-branch lines. Because of the large laser bandwidth (0.4 cm^{-1}) and predissociation broadening, most of the rotational states should have been detected. Although a slight detuning of the probe frequency did not affect the shape of the TOFMS profiles, a more detailed study would be desirable to fully characterize the degree (if any) of methyl rotational state selection in our measurements.

The principle of core-sampled TOFMS measurements has been described in detail by others [13–15]. Briefly, the expanded photofragment ion cloud is 'cored' by a small aperture in front of a microchannel plate detector. Only those photofragments with recoil velocity directed nearly parallel to the ion flight axis are detected, providing a near one-to-one correspondence between recoil velocity and ion flight time. In order to improve the energy resolution, it was desirable to operate the ion extraction optics in a delayed-pulse mode, where the common 'energy focussing' condition [16] is detuned so that the flight axis dimension of the photofragment sphere is elongated in space (and thus arrival time). The time (and thus energy) resolution in our experiments was limited by the large laser spot size. A time resolution of 20 ns was sufficient for the type of structure that we were interested in studying.

In order to compensate for the molecular beam velocity (which was perpendicular to the ion flight direction), it was necessary to offset the coring aperture by several millimeters from the centerline axis of the mass spectrometer. This condition was optimized by mounting the aperture on an xyz manipulator and maximizing the methyl REMPI signal from a sample gas which produced methyl radicals with a recoil energy distribution peaked near zero energy. Methyl radicals from multiphoton dissociative ionization of azomethane or methyl iodide served this purpose.

III. RESULTS AND DISCUSSION

A. Methyl Appearance Times

A knowledge of the timing between the loss of the two methyl radicals in azomethane is central to a proper mechanistic assignment. We have carried out a straightforward time delay measurement similar to that of the earlier CARS study [6], but now using 2+1 REMPI as the spectroscopic probe. Methyl ion signal was collected (without a coring aperture) and averaged by a boxcar integrator at 11 time delays between the dissociation laser and the REMPI probe laser. The results of this measurement are shown in Fig. 2 for the 0_0^0 and 2_1^1 methyl REMPI transitions. We obtained satisfactory fits with a rise time determined by the time profiles of the laser pulses, which suggests that the methyls in both vibrational states are lost on a much faster (subnanosecond) timescale.

Our result is quite different from that of the CARS experiments, which showed an appearance time of several nanoseconds for the vibrationless methyl. Our observation of subnanosecond appearance times for both methyl radicals is completely consistent with the concerted mechanism proposed by North *et al.* and corroborated by recent *ab initio* calculations, which predict a barrier to CH_3N_2 dissociation of less than 2 kcal/mol [1,17,18]. We note in particular that estimates of the dissociation lifetime, due to both tunneling and statistical mechanisms, range from 1 ns at the largest [17] to picoseconds or less [2,17,18]. Thus the balance of experimental and theoretical evidence provides little support for a CH_3N_2 lifetime in excess of a nanosecond.

An important caveat should be considered at this stage. We discuss later in more detail that we have probably measured only a limited subset of the total range of methyl quantum states produced in azomethane dissociation. Although the CARS measurements of the vibrational product state distribution did not show population in modes other than ν_2, the authors left open the possibility that not all Raman transitions had been found [7]. Indeed it would be rather surprising if the dissociation of azomethane produced excitation only in

the umbrella coordinate. For this reason, we cannot draw broad mechanistic conclusions based on our time delay measurements alone. Nor can we preferentially associate the states which we have observed with the primary or secondary steps of the dissociation. Instead, we note only that our measurements are *consistent* with the results of other studies which point more explicitly to a concerted process as the source for the majority of the reaction products [1,2].

Based on our methyl appearance time measurements alone, we cannot eliminate the possibility of a sequential mechanism on a timescale much shorter than a nanosecond. The secondary angular distribution measured by North *et al.* provides a more stringent upper limit on the lifetime and demonstrates that azomethane satisfies the common operational definition of a concerted dissociation, *i.e.* one where the intermediate survives for a time less than its rotational period. However, Kim *et al.* have noted in their ultrafast kinetics study of ketone dissociations [19,20] that an even more restrictive definition involves subpicosecond vibrational timescales. For acetone, they observed that a secondary dissociation lifetime of only 500 fs was still ten times slower than the primary dissociation. While this may reasonably be called a stepwise process, it would have been described as concerted based on the definition involving rotational periods [8,21].

In the end, a particular choice of the dividing line between concerted and stepwise is a matter of taste. The definitions which have been provided to date are based largely on measurable timescales of rotation or vibration. These processes reflect the torques and impulses (and thus the potential energy surface) of the dissociation, and they also depend strongly on mass factors. Alternatively, one could choose a criterion based exclusively on features of the potential energy surface. For the process $ABC \rightarrow AB + C \rightarrow A + B + C$, the dividing line might be drawn at coordinates beyond which the $AB + C$ interaction is less than some small fraction of its asymptotic value.

Whether ultrafast time-resolved measurements will prove useful for the azomethane system may depend on the dissociation mechanism. If the primary dissociation is fast, as it was in Kim's ketone study, the observation of different parent and intermediate lifetimes provides

direct evidence of a sequential mechanism. On the other hand, if the primary dissociation lifetime is much greater than the secondary, then sequential and concerted mechanisms become very difficult to distinguish experimentally, since the concentration of the intermediate can be negligibly small and the product appearance kinetics nearly identical for both mechanisms. $CH_3N_2^+$ and CH_3^+ ions produced by facile dissociative ionization of azomethane [9,11] may further complicate an MPI-based ultrafast study.

B. TOFMS Profiles

Correlated photofragment energy distributions can provide detailed information about the shape of the molecular potential energy surface. The goal of the experiments described in this section was to obtain translational energy distributions for methyl fragments with zero or one quantum of umbrella vibration. We measured core-sampled REMPI-TOFMS profiles for azomethane dissociation at 355 nm and at 330 nm. The measurements at the former wavelength allow a comparison with the results of North *et al.* and Weisman *et al.* The single-laser measurements at the latter wavelength allow comparison with the results of Fairbrother *et al.*, and confirms that the dynamics are virtually identical at this slightly higher energy.

Since a significant number of methyl ions are produced by nonresonant processes, it is necessary to subtract this background signal from the desired dissociation signal. (We actually subtract the corresponding translational energy distributions generated by fitting the data.) For each TOFMS profile collected with the probe laser tuned to a methyl resonance, we subsequently collected a background profile with the probe laser tuned between the 0_0^0 and 2_1^1 REMPI transitions. In order to average out some unavoidable slow drifts in experimental conditions, we collected many alternating on- and off-resonance profiles for 5–10 minutes each. Typical experimental conditions produced less than one core-sampled ion per laser shot. Figs 3 and 4 show TOFMS profiles and corresponding translational energy distributions for dissociation at 355 nm and 330 nm (more precisely, at the REMPI transition

frequency), respectively. The upper and lower traces within each frame correspond to the on- and off-resonance signals, respectively.

We fit the profiles by forward convolution of optimized translational energy distributions, using a standard simplex routine to minimize the squared residuals. The distributions were a sum of 'prior'-like functions with the form $(E/E_{max})^a(1 - E/E_{max})^b$, where E_{max} is the maximum possible translational energy permitted by energy conservation, and a and b are adjustable parameters [22]. Each off-resonance background profile was fit with a single such component. The on-resonance profiles were each fit with one component identical to the background profile fit, and two additional components of the same functional form, each with independently adjustable exponents a and b and relative weighting factors. We have chosen this functional form only for its flexibility and not to imply a particular mechanistic interpretation. Detailed interpretations or the choice of a more complex functional form would not be very meaningful given the moderate scatter in the data.

The true translational energy distributions, obtained by subtracting the off-resonance from the on-resonance distributions, appear in Fig. 5 for both dissociation wavelengths. Three coarse features of these distributions deserve emphasis. First, they all show bimodal structure, with one component peaked below 10 kcal/mol, and the second peaked between 10–20 kcal/mol. Although local minima in the total residual exist for fits in which a single adjustable component dominates, these residuals were always higher than for fits obtained with two adjustable components. The second important feature of the distributions is their similarity for the two methyl quantum states. The small differences between the 0_0^0 and 2_1^1 data in Figs 3 and 4 are not significant when the data scatter is considered. Third, the distributions from 355 nm and 330 nm dissociation are qualitatively similar. This is not surprising, since only a small fraction of the energy difference between the two wavelengths (6 kcal/mol) is expected to appear in translation. However, since our energy scale calibration may have varied by as much as 10% over the course of several days of data collection, any such differences in translational energy release would not be clearly identifiable.

Our translational energy distributions should be compared to the results of North *et al.*

[2] and Fairbrother *et al.* [9]. North's distribution (quantum-state-averaged) is reproduced in Fig. 6, and shows distinct features peaking at 14 kcal/mol and 5 kcal/mol. The peak energies of the two components in our distributions are very similar to those in Fig. 6, although the components are broader, and their relative weightings are much different. These differences do not necessarily imply that the measurements disagree, however, since we have measured only a small (and possibly extreme) subset of methyl quantum states, and partitioning into translation is likely to vary with the fragment internal states. Indeed, one major objective of this work is to investigate such differences.

Our results agree qualitatively with those of Fairbrother *et al.*, although our quantitative conclusions are less extreme. They reported an exclusive preference for North's high energy component in their measurements of non-core-sampled TOFMS profiles for the same methyl quantum states. In their analysis, they did not attempt to fit their TOFMS profiles, but were able to extract an average translational energy of 15.8–17.4 kcal/mol. In contrast, the average energies of our distributions are slightly lower (14.3–15.3 kcal/mol), consistent with our observation of an additional component at lower energies. A thorough appraisal of their conclusions is not possible without knowing more details of their analysis, but the conclusion of high selectivity for the fast component seems overly strong and does not agree quantitatively with our observations.

From their measurements of appearance times and state distributions, Weisman *et al.* reached an indirect conclusion on energy partitioning in the umbrella mode [6,7], which was much different than our direct observations. They proposed that the first methyl departs impulsively, while the second is lost in a statistical manner. However, their assignment of vibrationless methyls to the second step directly contradicts our observation that the vibrationless methyls are predominantly fast, which would be expected for an impulsive process. The explanation for this discrepancy is probably related to the fact that their interpretation relies heavily on the appearance time measurements, which are also at odds with our observations.

Two features of our results require further discussion—the non-dependence on vibrational

state and the favoring of faster energies in comparison to the results of North *et al.* At this stage we provide qualitative arguments, but in the future, classical trajectory simulations on the recent *ab initio* potential energy surfaces [1] would be extremely valuable for verifying or disproving these propositions. In principle, extensive experimental measurements of correlated energy distributions should permit one to confirm or reject the present interpretation of a statistical dissociation with an exit barrier. However in the present study, since we have observed only a limited fraction of the fragment quantum states, we avoid drawing broad conclusions about the global dynamics.

A simple calculation by North and Gezelter [21,23] shows that such caution is necessary and also suggests an explanation for the similar translational energy distributions of both methyl vibrational states. Their model addresses statistical dissociations with an exit barrier: energy in excess of the dissociation barrier is partitioned statistically, while the remaining fraction is released impulsively by the exit barrier. For azomethane, they further assume that the first methyl is lost with no exit barrier and only the second has an impulsive component. This model yields average vibrational energy in the first and second methyls of 8.2 kcal/mol and 9.9 kcal/mol, respectively, with both values dominated by the statistical partitioning in the highly excited azomethane parent. In fact, it is generally true that statistical partitioning of a large excess energy will leave substantial vibrational energy in most of the fragments.

Most of the methyl radical fragments would therefore be found in vibrational states other than the two which we have measured (one quantum of ν_2 is only 606 cm^{-1} or 1.73 kcal/mol). It would not be surprising for this limited subset of photofragments to have translational energy distributions much different than the internal-state-averaged distributions measured by North *et al.* Whether a methyl fragment has zero or one quantum of umbrella vibration probably matters less than the fact that both types are near the same extreme with respect to average vibrational energy. For these reasons, our results are consistent with the dissociation mechanism proposed by North *et al.* and Liu *et al.* to explain North's experimental observations. On the other hand, a proposed mechanism which predicts low average vibra-

tional energies, where our distributions would be more representative of the average, would be more difficult to reconcile with the state-averaged measurements.

The total methyl translational energy distribution of Fig. 6 contains roughly equal contributions from 'fast' and 'slow' components. In contrast, our distributions strongly favor the 'fast' component—thus the low energy wing of the methyl vibrational energy distribution ($\nu_2 = 0, 1$) appears to correlate with the higher energy region of the total methyl translational energy distribution. Although such a negative correlation is predicted by statistical models, we observe a much stronger correlation than would be expected for a purely statistical dissociation: one expects the vibrational energy *deficit* (5-10 kcal/mol here, with respect to the calculated average [23]) to be distributed among many degrees of freedom, yet we see a comparable energy increase in the methyl translational degree of freedom alone. Because of the large exit barrier, azomethane is expected to deviate significantly from statistical behavior, even if internal energy is largely randomized prior to dissociation. Indeed, the fact that the translational energy distributions peak strongly away from zero energy clearly reflects non-statistical behavior. Further theoretical work and more extensive quantum-state-resolved measurements will be necessary to further clarify the influence of the exit barrier.

IV. CONCLUSION

The ultraviolet dissociation of azomethane continues to be a rich source of insight into three-body dissociation dynamics. Our observation of laser-limited appearance times for both vibrationless and umbrella-excited methyl photofragments provides further evidence that azomethane dissociation is dominated by a concerted mechanism rather than a sequential mechanism. The correlated vibrational-translational energy distributions for the methyl fragments have opened a small but revealing window into the finer details of azomethane dissociation. The bimodal structure of the distributions agrees with earlier state-averaged measurements, though the widths and relative intensities of the two components differ. These differences do not imply a contradiction, since a limited subset of fragment quantum

states were probed in the present study. Our translational energy distributions are thus consistent with the previously proposed mechanism of energy scrambling followed by concerted dissociation, however, classical trajectory simulations are needed for a more complete understanding of the detailed processes involved. The inherent complexity of the three-body process is further complicated by the experimental challenge of a low absorption cross section and relatively efficient multiphoton absorption. It will not be a small task to study a wider range of fragment quantum states or ultrafast kinetics, however the results should be very rewarding.

ACKNOWLEDGMENTS

This work was supported by the Director, Office of Energy Research, Office of Basic Energy Sciences, Chemical Sciences Division, of the U.S. Department of Energy under Contract No. DE-AC03-76SF00098.

REFERENCES

[1] R. Liu, Q. Cui, K.M. Dunn, and K. Morokuma, J. Chem. Phys. **105**, 2333 (1996).

[2] S.W. North, C.A. Longfellow, and Y.T. Lee, J. Chem. Phys. **99**, 4423 (1993).

[3] G. Kortum and H. Rau, Ber. Buns. **68**, 973 (1964).

[4] M.B. Robin, R.R. Hart, and N.A. Kuebler, J. Am. Chem. Soc. **89**, 1564 (1967).

[5] O.A. Mosher, M.S. Foster, W.M. Flicker, J.L. Beauchamp, and A. Kuppermann, J. Chem. Phys. **62**, 3424 (1975).

[6] K.A. Burton and R.B. Weisman, J. Am. Chem. Soc. **112**, 1804 (1990).

[7] B.K. Andrews, K.A. Burton, and R.B. Weisman, J. Chem. Phys. **96**, 1111 (1992).

[8] C.E.M. Strauss and P.L. Houston, J. Phys. Chem. **94**, 8751 (1990).

[9] D.H. Fairbrother, K.A. Dickens, P.C. Stair, and E. Weitz, Chem. Phys. Lett. **246**, 513 (1995).

[10] T. Gejo, P. Felder, and J.R. Huber, Chem. Phys. **195**, 423 (1995).

[11] A.S. Bracker, D.A. Blank, S.W. North, A.G. Suits, and Y.T. Lee, Manuscript in Preparation .

[12] J.W. Hudgens, T.G. DiGiuseppe, and M.C. Lin, J. Chem. Phys. **79**, 571 (1983).

[13] R. Ogorzalek Loo, H.-P. Haerri, G.E. Hall, and P.L. Houston, J. Chem. Phys. **90**, 4222 (1989).

[14] J.A. Syage, J. Chem. Phys. **105**, 1007 (1996).

[15] W.R. Simpson, A.J. Orr-Ewing, T.P. Rakitzis, S.A. Kandel, and R.N. Zare, J. Chem. Phys. **103**, 7299 (1995).

[16] W.C. Wiley and I.H. McLaren, Rev. Sci. Inst. **26**, 1150 (1955).

[17] B.K. Andrews and R.B. Weisman, J. Chem. Phys. **101**, 6776 (1994).

[18] C.H. Hu and H.F. Schaefer III, J. Phys. Chem **99**, 7507 (1995).

[19] S.K. Kim, S. Pederson, and A.H. Zewail, J. Chem. Phys. **103**, 477 (1995).

[20] S.K. Kim and A.H. Zewail, Chem. Phys. Lett. **250**, 279 (1996).

[21] S.W. North, *Photofragment Translational Spectroscopy of Three Body Dissociations and Free Radicals*, PhD thesis, University of California, Berkeley, 1995.

[22] S.W. North, A.J. Marr, A. Furlan, and G.E. Hall, J. Phys. Chem. **101**, 9224 (1997).

[23] S.W. North, D.A. Blank, C.A. Longfellow, J.D. Gezelter, C.A. Longfellow, and Y.T. Lee, J. Chem. Phys. **102**, 4447 (1995).

FIGURES

FIG. 1. Schematic azomethane potential energy curves, adapted from Ref. [1]. Concerted, synchronous, and sequential mechanisms are discussed in the text.

FIG. 2. Dependence of CH_3 REMPI signal on time delay between pump and probe lasers, for 0_0^0 and 2_1^1 transitions. Appearance times are laser pulsewidth-limited and equivalent for both vibrational states. The REMPI signal is offset from zero due to dissociation by the probe laser and to a lesser extent (<20%) from nonresonant multiphoton processes (see text for details).

FIG. 3. Methyl REMPI-TOFMS profiles (with fits) and corresponding translational energy distributions for 355 nm dissociation of azomethane, 0_0^0 and 2_1^1 REMPI transitions. The lower trace in each frame correponds to off-resonance background signal.

FIG. 4. Methyl REMPI-TOFMS profiles (with fits) and corresponding translational energy distributions for 330 nm dissociation of azomethane (single laser for dissociation and probe), 0_0^0 and 2_1^1 REMPI transitions. The lower trace in each frame correponds to off-resonance background signal.

FIG. 5. Translational energy distributions for 355 nm and 330 nm dissociation of azomethane, obtained by subtracting on- and off-resonance distributions of Figs 3 and 4. Sold lines are for 0_0^0 data, dashed lines for 2_1^1 data.

FIG. 6. Translational energy distribution from Ref. [2] for methyl photofragments (all quantum states).

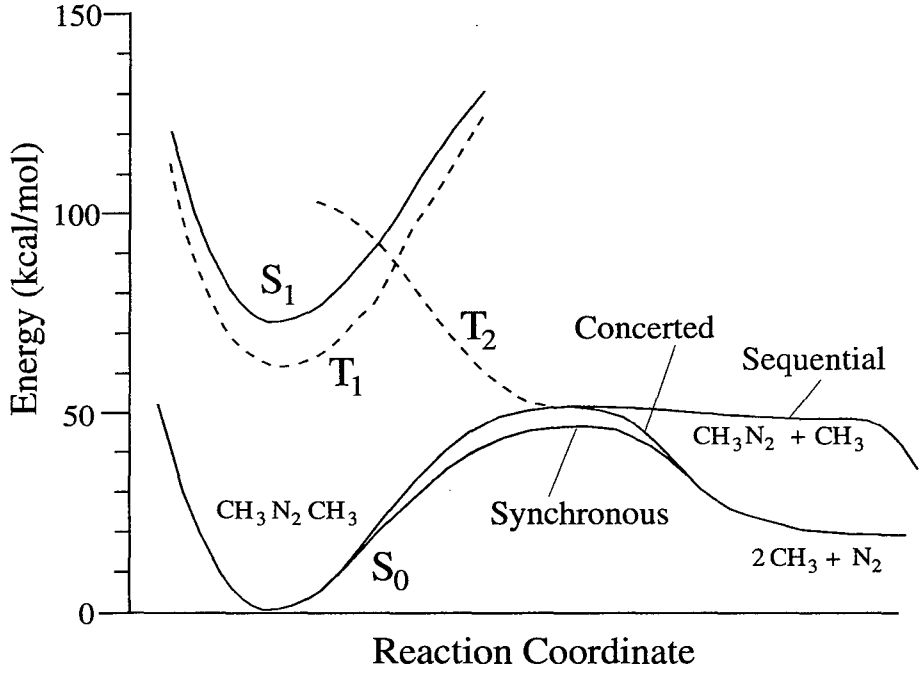

Figure 1, Bracker et al. submission to Journal of Chemical Physics

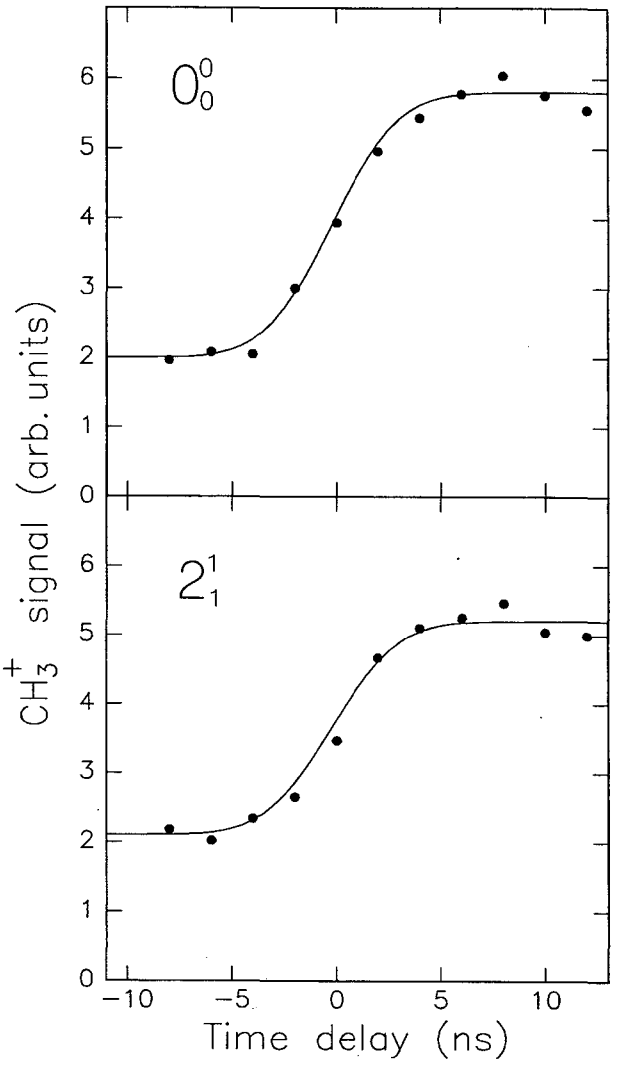

Figure 2, Bracker et al. submission to Journal of Chemical Physics

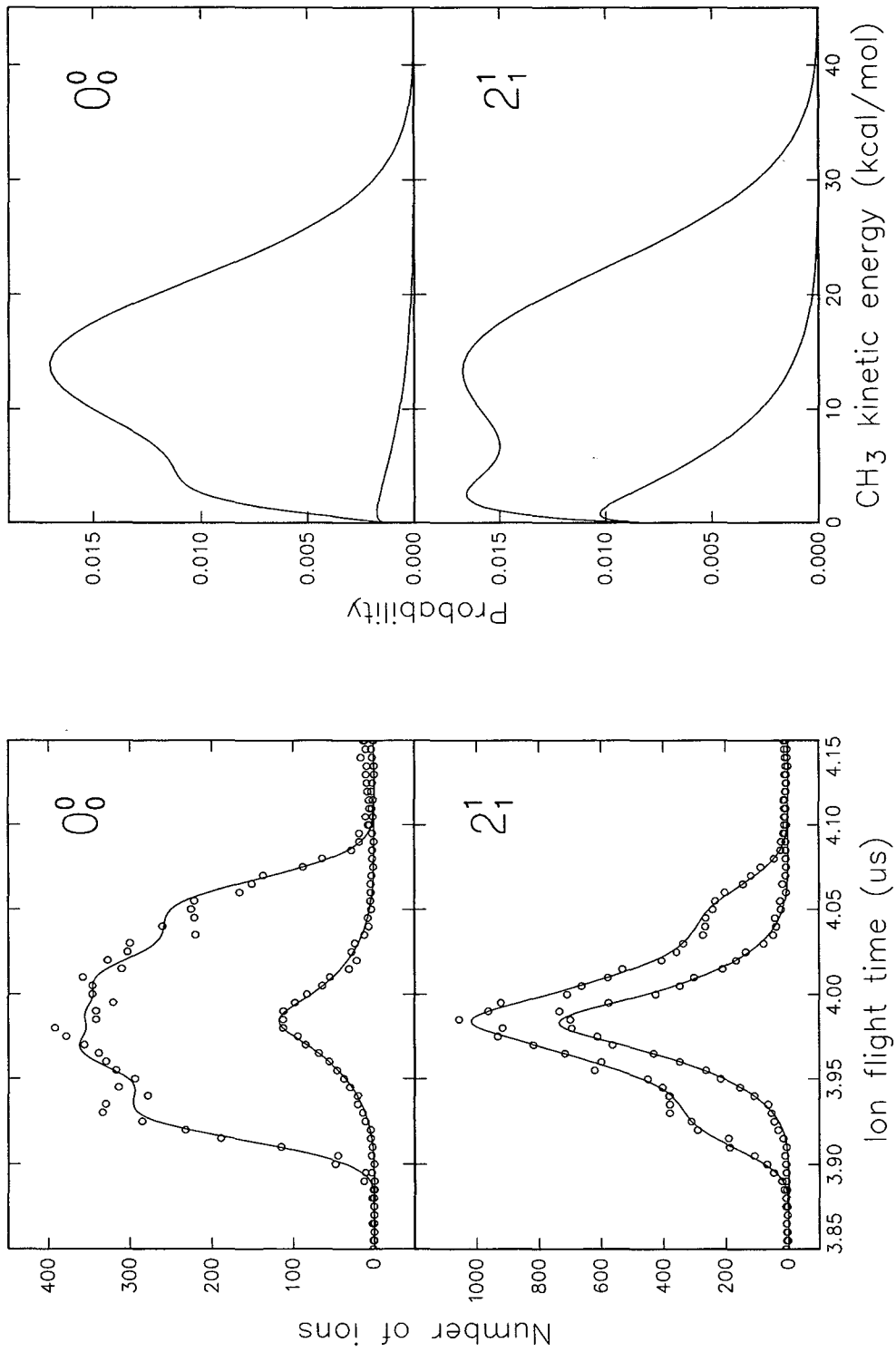

Figure 3, Bracker et al. submission to Journal of Chemical Physics

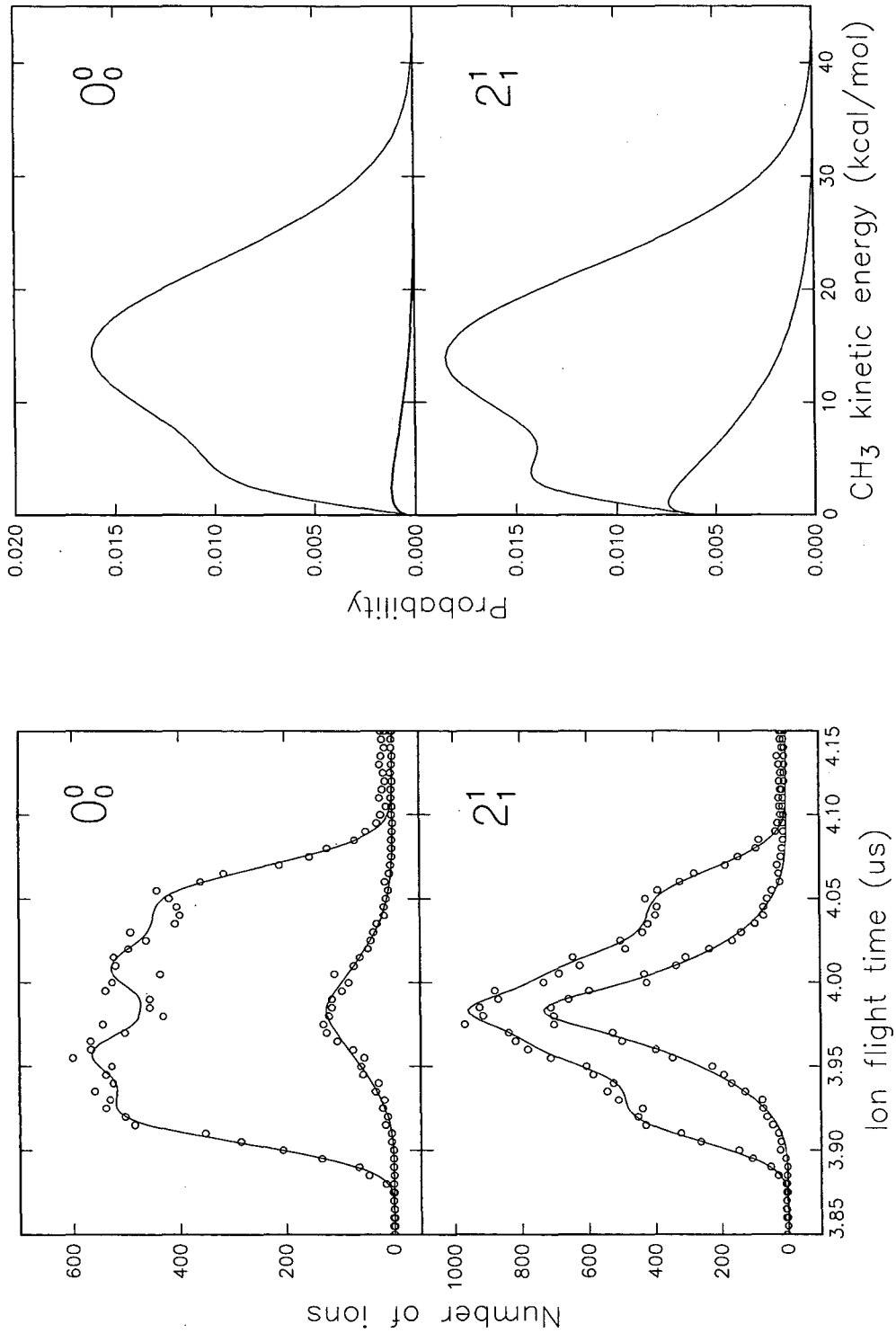

Figure 4, Bracker et al. submission to Journal of Chemical Physics

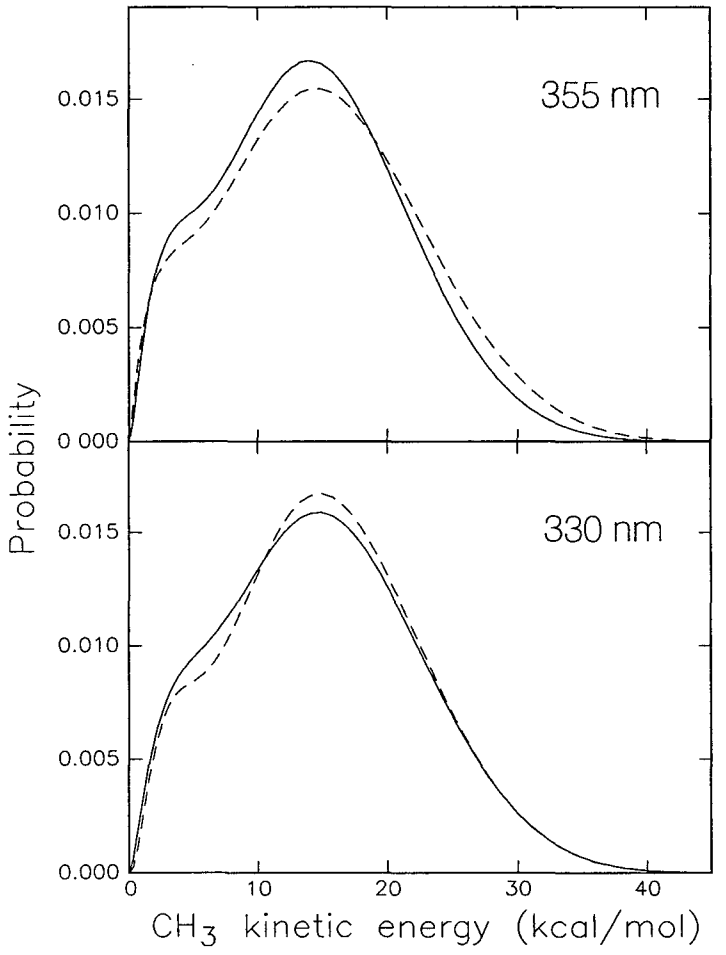

Figure 5 , Bracker et al. submission to Journal of Chemical Physics

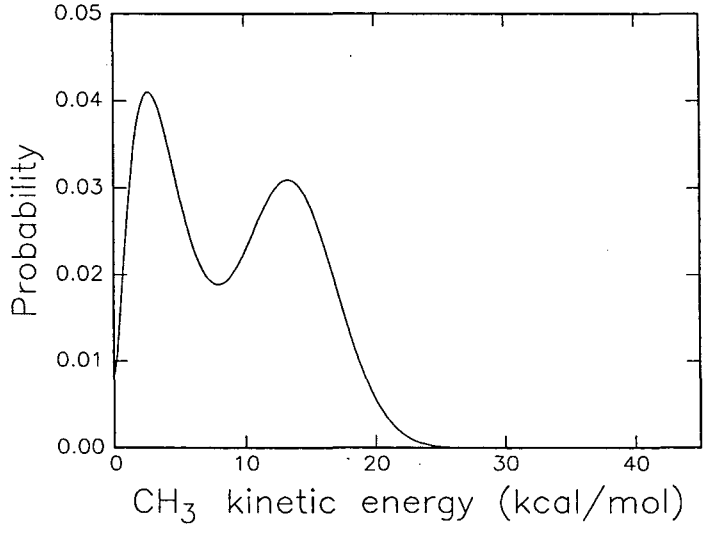

Figure 6, Bracker et al. submission to Journal of Chemical Physics

Ernest Orlando Lawrence Berkeley National Laboratory
One Cyclotron Road | Berkeley, California 94720

Prepared for the U.S. Department of Energy under Contract No. DE-AC03-76SF00098